Optik - International Journal for Light and Electron Optics 315 (2024) 172040

Contents lists available at ScienceDirect

Optik

journal homepage: www.elsevier.com/locate/ijleo

A closely spaced dual band polarization insensitive FSS for 5G applications

Sibel Ünaldı [a,*], Nigar Berna Teşneli [b]

[a] Department of Electrical and Electronics Engineering, Faculty of Engineering, Bilecik Şeyh Edebali University, Bilecik TR11100, Turkiye
[b] Department of Engineering Fundamental Sciences, Sakarya University of Applied Sciences, Sakarya, Turkiye

ARTICLE INFO

Keywords:
Closely spaced
Dual band
FSS
Polarization-insensitive
5G
Stop band

ABSTRACT

This study presents a novel single layer Frequency Selective Surface (FSS) for fifth generation (5G) applications with a polarization independent closely spaced dual band response. The proposed design consists of four split ring apertures etched on a square patch printed on a RT5880 dielectric substrate. The FSS has two stop-bands at 24.78 GHz and 28 GHz center frequencies with attenuations around 55 dB. The S21<−10 dB bandwidths (BW) of these bands are 14.48 % and 9.25 %, respectively and these closely spaced bands succeed 1.13 frequency ratio. It shows a stable frequency response for both TE and TM polarizations. Furthermore, the FSS represents a single layered and quite thin (thickness $0.042\lambda_l$) structure with its unit cell size ($0.70\lambda_l \times 0.70\lambda_l$, where λ_l is the free-space wavelength at lower frequency). The novelty of the presented FSS is not only achieving a small closely spaced band ratio in the mmWave band and exhibiting polarization insensitivity but also providing these features with a simple geometry and, uncomplicated single layer structure. The simulation results were confirmed by well accordant measurement results. All these results make the presented FSS a good candidate for 5G electromagnetic interference (EMI) shielding applications.

1. Introduction

Wireless communication technologies have evolved at an inconceivable speed until today and the developments still continue unabated. These innovations bring to wireless networks advanced requirements such as massive data volumes, huge data transfer rates, spectacular coverage, and ultra-dense parallel communications. To fulfill these demands, advancing to 5th generation (5G) wireless systems is inevitable. This circumstance accelerates the research about 5G technologies and applications on one hand, it also commenced the frequency band deployment for future wireless networks on the other hand [1]. 5G NR (New Radio) is the new radio access technology proposed by the 3rd Generation Partnership Project (3GPP) and designed to establish a standard for a more capable 5G wireless air-interface [2–4]. 5G NR frequency bands are involved in the 3GPP TS 38.101 [5]. 5G NR frequency bands use two frequency ranges in general; Frequency Range 1 (FR1) and Frequency Range 2 (FR2). FR1 includes sub-6 GHz frequency bands whereas FR2 includes frequency bands in the millimeter wave (mmWave) range. Even if the use of FR1 seems more practical it should be rearranged for 5 G as this region is already in use for previous standards, while the mmWave region offers empty bands suitable for use. mmWaves, interjacent between microwaves and infrared waves, are accepted to be an important spectrum region for the 5G. Although the 26, 28, 38, and 60 GHz bands are widely studied [6], most of the current research and pioneer 5G applications are

* Corresponding author.
E-mail addresses: sibel.unaldi@bilecik.edu.tr (S. Ünaldı), btesneli@subu.edu.tr (N.B. Teşneli).

https://doi.org/10.1016/j.ijleo.2024.172040
Received 7 July 2024; Received in revised form 21 August 2024; Accepted 14 September 2024
Available online 16 September 2024

concentrated on the 24.25–29.5 GHz mmWave frequency range. This region covers the n257 (26.5–29.5 GHz), n258 (24.25–27.5 GHz), and n261 (27.5–28.35 GHz) bands of 5 G NR. However, the mmWave spectrum has some critical issues that must be overcome for efficient mobile communications.

Frequency Selective Surfaces (FSSs) are periodically engineered structures to generate bandpass or bandstop frequency response [7, 8]. FSSs, which are often used in conjunction with antennas, are started to design for 5G frequency bands recently [9]. Dual-band or multi-band communication applications constitute a significant part of recent wireless communication devices. Some recent works on dual-band FSS designs for 5G bands are present [10–13]. Further, the FSSs functioning properly in dual or multi bands with good band isolation in 5G frequency bands are another important requirement. There are also several studies that closely located dual or triple band FSSs have been reported in the literature [14–19]. But in most designs, proposed frequency bands are in the sub-6 GHz regions. The designs in [20] and [21] present dual band responses in different band regions, one is at mmWave region and the other is at lower frequencies. The authors of the [22] have presented a miniaturized FSS with four narrow pass bands in the 0–30 GHz range, but only one of these bands exists above the 20 GHz region. Ref. [23], proposed a closely settled dual band FSS operating at mmWave bands. In the study, the band ratio of the proposed multi-layered FSS has been stated as 1.16. In ref. [24] a closely spaced tri band FSS was proposed resonating at 19.52 GHz, 23.6 GHz, and 31.2 GHz frequencies. Although the FSSs in the last two mentioned studies presented closely located bands in the mmWave region, they were able to achieve this with multilayer structures that are relatively thick for most applications. This discussion shows that designing a single-layer, dual-band or multiple-band transmission block FSS with a very small band ratio and simple geometry is still a challenging task. Band-stop FSSs, which block certain frequency regions and provide high Shielding Effectiveness (SE), are good options for EMI shielding applications as they allow out-of-band frequencies to propagate instead of blocking the entire EM waves like metal shields. In this study, a novel, single-layer, polarization independent transmission block FSS is proposed with simple geometry. The presented FSS has stop bands at 24.78 GHz and 28 GHz. The band ratio of these closely spaced bands is only 1.13. The proposed structure is the one in the literature to the best of our knowledge, with its band ratio in the 24.25–29.5 GHz mmWave frequency range.

2. Unit cell design and simulation results

Closely spaced frequency band allocations in wireless communication systems can lead to electromagnetic interference. Dual-band FSSs with closely spaced transmission bands can provide adequate band isolation to prevent interference between systems operating in nearby frequency bands. To achieve close resonances in the frequency response of the FSSs, multilayer structures or fractal geometries are generally used in the designs. However, complex geometries may require more sensitive manufacturing techniques. The resonant frequency band ratio is defined as the ratio of the higher to the lower one (f2/f1) of two consecutive resonant frequencies in the FSS frequency response and generally, is used as a figure of merit to indicate closely spaced bands for dual or multi-band FSSs. In this study, a single layer FSS with closely spaced and polarization stable frequency response is designed. The geometry of the proposed FSS is intended to work in the 5 G frequency band between 24.25–29.5 GHz. The designed unit cell with the dimensions is depicted in Fig. 1. It consists of a square patch, and four split rings aperture to achieve desired frequency coverage in a closely spaced dual band.

The final dimensions, optimized to obtain the desired operational frequency band of the transmission coefficient, being less sensitive to manufacturing tolerances, are D=8.5 mm, g=0.38 mm, k=5.57 mm, Ri=0.58 mm, Ro=0.96 mm. There is a distance of 1.63 mm between the center of each split ring aperture and the center of the unit cell/square patch.

The presented unit cell structure is designed on a RT5880 dielectric substrate with a dielectric constant of 2.2 and a thickness of 0.508 mm. The overall size of the proposed unit cell is 8.50 mm × 8.50 mm ($0.70\lambda_l \times 0.70\lambda_l$, where λ_l is the free-space wavelength at the lower frequency of 24.78 GHz).

The designed FSS has a simple geometry that is printed on a single-layer substrate. The simple structure of the proposed FSS ensures an easier manufacturing process and lower cost, and thus preferability for practical applications. The highlight of the designed FSS is exhibiting close located dual stopbands at 24.78 and 28 GHz frequencies with a high transmission blocking feature. Additionally, the symmetrical structure of the unit cell supports the stable frequency response for both TE and TM polarizations.

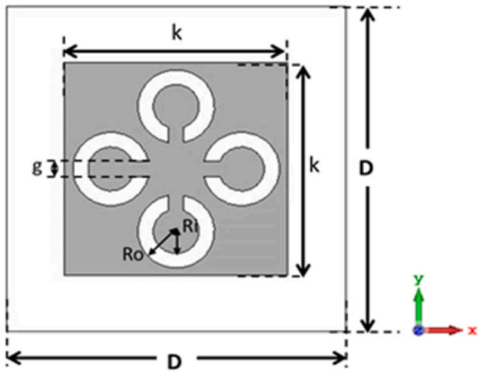

Fig. 1. Schematic of the designed unit cell with dimensions.

The design procedure of the proposed unit cell structure consists of 4 steps which are illustrated in Fig. 2. The first step is a simple square patch that has a frequency response at 29.72 GHz. The frequency response of the FSS is shifted towards the targeted frequency region by adding ring apertures to the structure with the 2nd and 3rd steps. Finally, a metallic split is adopted to each ring aperture and the proposed FSS is attained. Dual-band band-stop response is obtained by implementing metallic splits to ring apertures at the final evolution step. The transmission characteristics of the four evolution step of the unit cells (a, b, c, and the proposed unit cell) are depicted comparatively in Fig. 3.

One of the most important parameters affecting the frequency response is the width of the ring apertures (Ro-Ri). This value has been controlled by the inner radius of the ring apertures in the design process. As the ring apertures are broaden both transmission zeros shift slightly to the higher frequencies, but this change causes more noticeable frequency shift in the first band than in the second one. The presented band ratio is optimized with the width of the ring apertures. A parameter analysis for different values of (Ro-Ri) is shown in Fig. 4. Obtained band ratio according to this parameter analysis are 1.19 (Ro-Ri=0.2), 1.17 (Ro-Ri=0.3), 1.13 (Ro-Ri=0.4), and 1.13 (Ro-Ri=0.5).

The transmission blocking mechanism of the proposed FSS can be explained by the equivalent circuit model (ECM). In ref [25] an ECM has been proposed for four circular loop apertures with reporting good results. The presented FSS will have a similar equivalent circuit as it includes four circular loop apertures. But it requires a small arrangement due to the implemented metallic splits to ring apertures. The patch of the resonator acts as an inductance (L1) and the included apertures behave like a parallel capacitance (C1) with (L1). Thus the frequency of transmission zeros can be expressed with the well-known expression $1/2\sqrt{L1C1}$. But an additional inductance (L2) series to (C1) have to be introduced because of the constituted metallic splits in the apertures. The metallic splits included in the apertures cause also the existence of the new capacitive parts (C2). This gives rise to splitting the resonance band and the transition of single band to dual band response. Since the width of the ring apertures is effective on both the values of C1 and C2, it is a key parameter for tuning the close located bands. As a result, a dual-band response is achieved at 24.78 GHz and 28 GHz with the $S21<-10$ dB BWs of 14.48 % and 9.25 %, respectively, and well transmission-blocking feature. Besides, a narrow passband comprises with a fractional BW of 5.12 % between these closely located stopbands. Fig. 5.(a) illustrates the inductive and capacitive parts for the proposed FSS for the TE polarization along the *y*-axis and Fig. 5.(b) depicts the adopted equivalent circuit model for the inductive and capacitive components belonging to the constituent parts of the unit cell.

Fig. 6 shows the surface current distributions on the FSS under TE and TM polarized EM wave incidence at both transmission zeros. For TE polarization, a higher surface current density exists along the vertical split ring apertures and vertical edges of the resonator, while the surface currents are concentrated on the horizontal elements of the resonator in TM polarization. Current flows along the outer perimeter of the ring apertures for the transmission zero at 24.78 GHz, whereas current flow occurs along the inner perimeter of the ring apertures with a shorter path at 28 GHz. Moreover, the current flow in opposite directions around the circular ring apertures points out the capacitive effect illustrated in Fig. 6. A 90^o phase difference on surface current distributions for both polarizations can be seen clearly from Fig. 6.

Fig. 7 shows the simulation results of the reflection and transmission coefficients of the proposed design for TE and TM polarizations under normal incidence. For the two stop bands of the presented FSS, the band ratio was obtained as a very low value of 1.13. The transmission and reflection characteristics of the designed FSS exhibit a passband with 26.5 GHz center frequency and −0.24 dB insertion loss (IL) between the two transmission blocks. The structure realizes a reflection to transmission band ratio (f_r /f_t) of 0.94, which is also very less. As seen in Fig. 7, stable frequency response is achieved in both polarizations. The identical filter response for both TE and TM polarizations is provided by the symmetrical geometry of the presented unit cell with respect to the 90° rotations around the axis passing through its center.

3. Fabrication and measurement

The presented structure is fabricated and measured for validation of the obtained simulation results. The fabricated FSS prototype with a square patch and four split rings aperture is built on a Rogers RT5880 substrate with the dielectric constant of ε_r=2.20 and a thickness of 0.508 mm. The designed FSS is fabricated as a 26 × 17 array on a 228.6 mm × 152.4 mm dielectric panel. In Fig. 8(a), a fabricated prototype of the designed FSS is illustrated with an enlarged view.

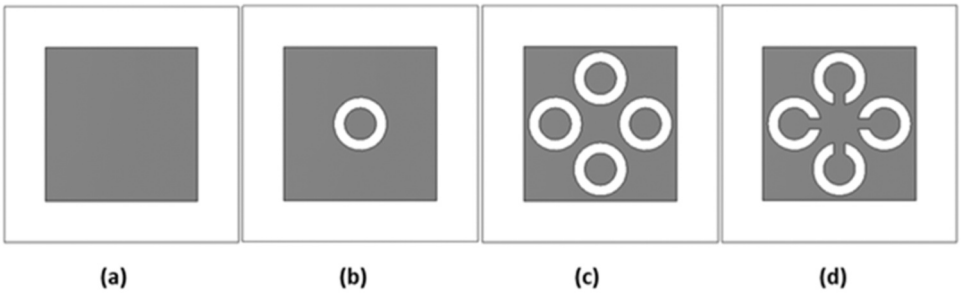

Fig. 2. Schematic Design steps **(a)** square patch, **(b)** square path and a ring aperture, **(c)** square path and four rings aperture, **(d)** square patch and four split rings aperture (proposed design).

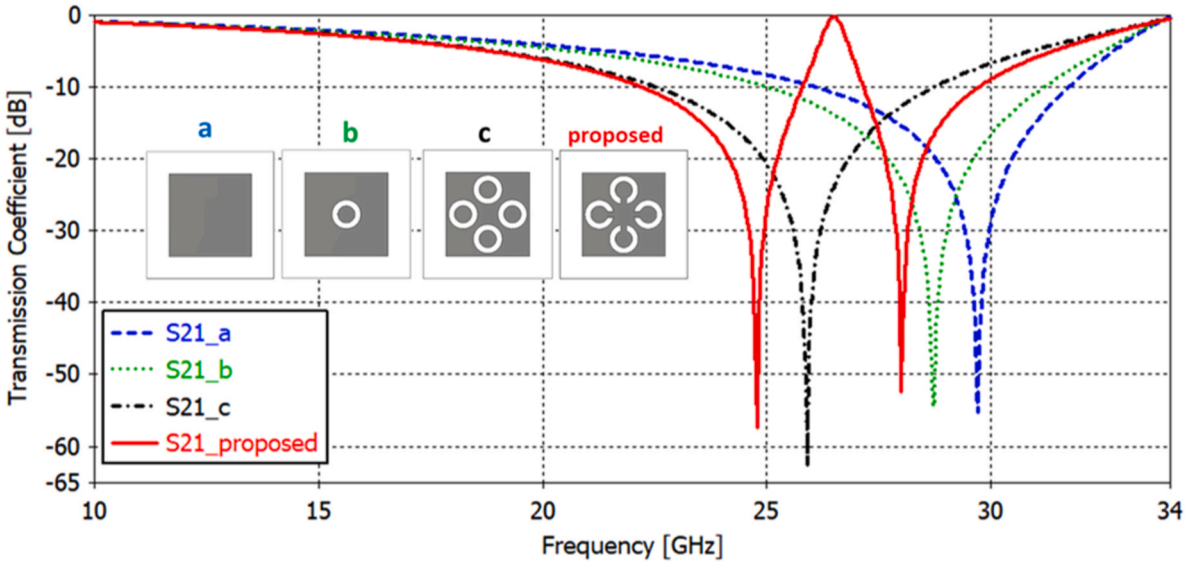

Fig. 3. Simulation results for the transmission coefficients of each design steps.

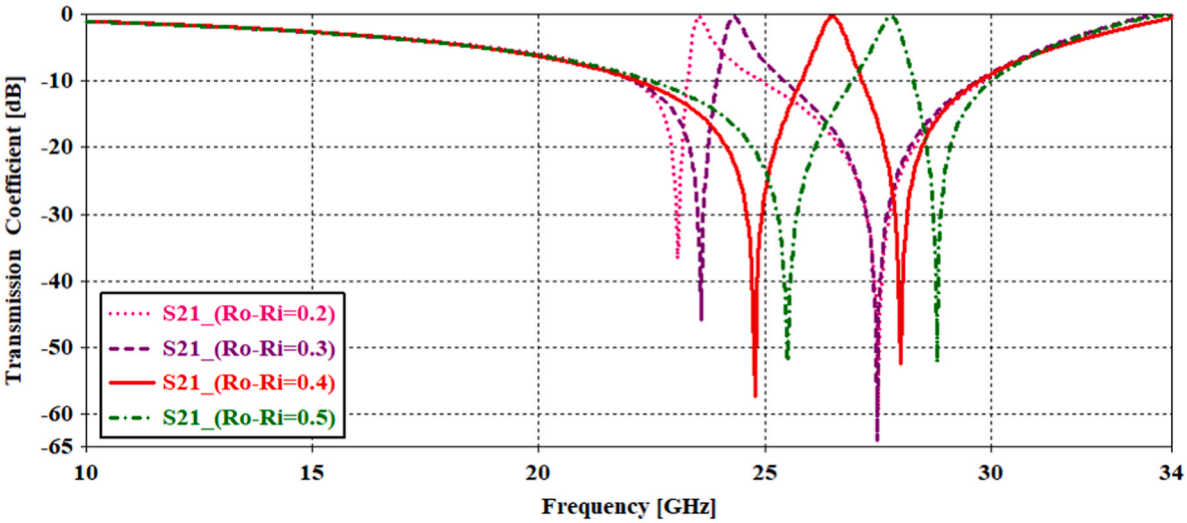

Fig. 4. Simulation results of the transmission coefficients for different (Ro-Ri) values.

The frequency responses of the fabricated prototype are measured using the Agilent E8363B Network Analyzer and two horn antennas. The excitation port of the VNA is connected to the transmitting (Tx) horn antenna by a coaxial cable and the receiving (Rx) horn antenna is connected to the other port of the VNA. Then the FSS is placed between them by fixing with a foam fixture and putting to an aperture with the same size as the prototype. The distance between the horn antenna and FSS is adjusted as $>2D^2/\lambda$, where λ is the operation frequency and D is the FSS periodicity so that the plane wave incidence on the FSS is assured. The measurement set up to determine the transmission coefficient of the FSS is shown in Fig. 8(b). The measurement process of the FSS has two steps. The first step is the calibration, comprising measurement of the transmission coefficient of the test environment without the fabricated prototype and the second step includes measurement of the fabricated prototype and evaluation of the results with considering the difference between the two measured values.

The comparison of the simulation and measurement data of the designed FSS under normal incidence is depicted in Fig. 9. The simulation and experimental results exhibit satisfying agreement. The measured transmission zeros are obtained at 24.64 GHz and 28.21 GHz, whereas the simulated ones are at 24.78 GHz and 28 GHz, respectively. The boundaries for the −10 dB limit of the stopbands are occurred between 22.24 GHz-26.24 GHz and 27.50 GHz - 29.83 GHz frequencies with a small deviation respect to the simulation results. The edge diffraction due to the finite unit cell number of the prototype, fabrication imperfections and measurement tolerance can give rise to this slight shift. Also, it supports that the designed geometry provides polarization independence.

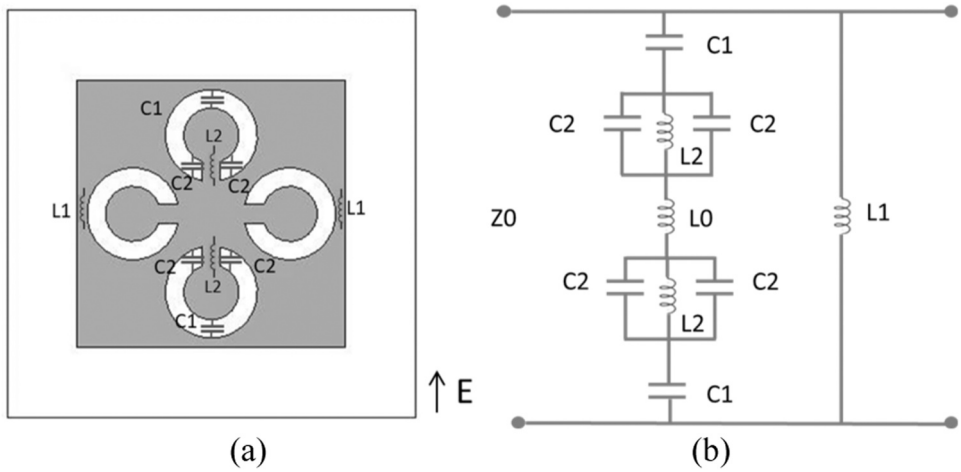

Fig. 5. (a) The inductive and capacitive parts of the proposed FSS, (b) The ECM of the proposed FSS.

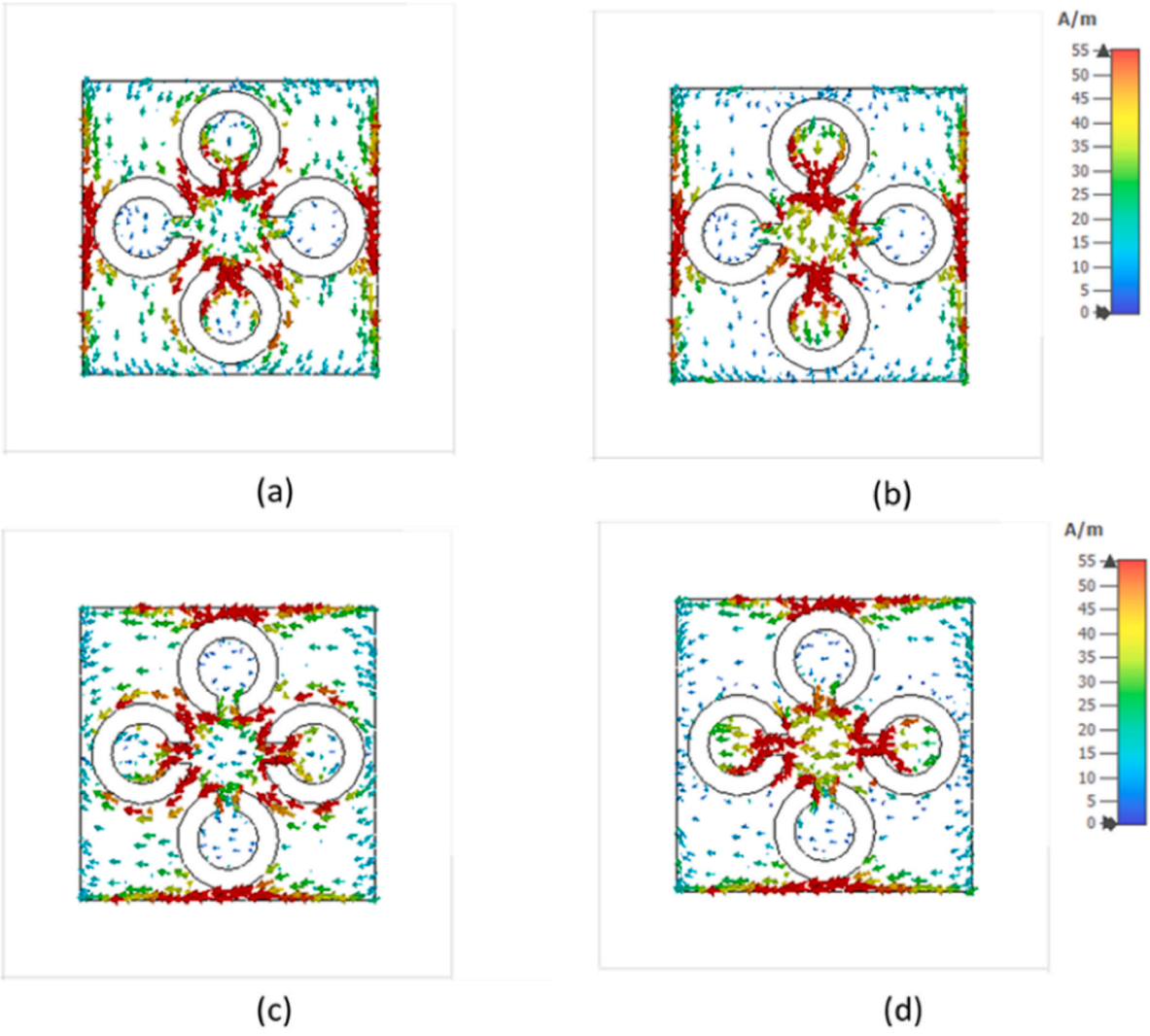

Fig. 6. Surface current distributions of the FSS for TE mode at (a) 24.78 GHz, (b) 28 GHz; for TM mode at (c) 24.78 GHz, and (d) 28 GHz.

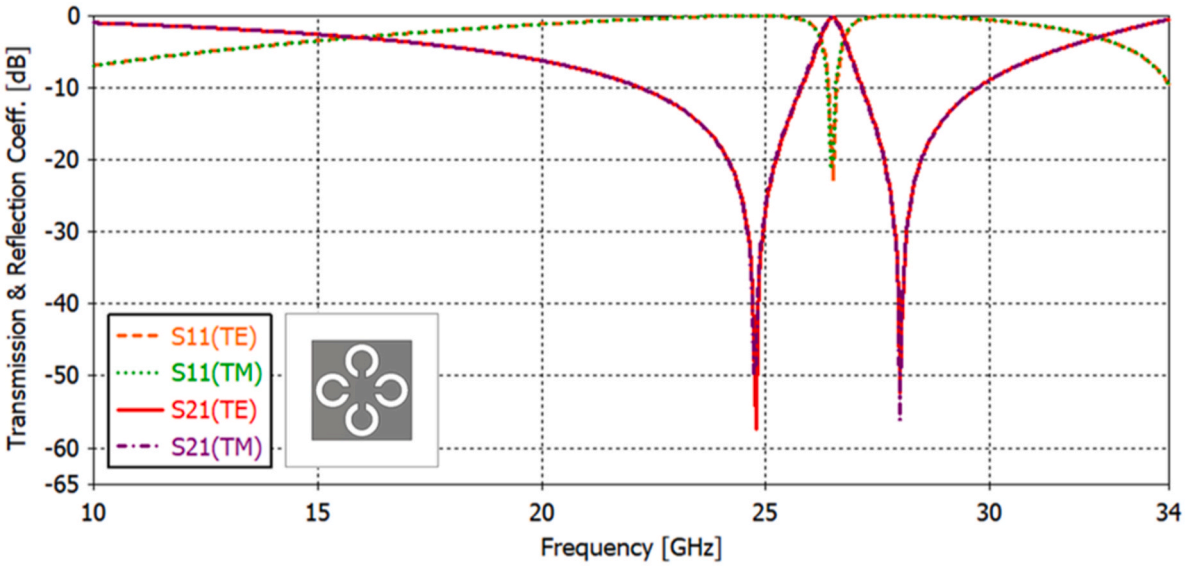

Fig. 7. Simulation results of the transmission and reflection coefficients of the proposed design for both TE and TM polarizations.

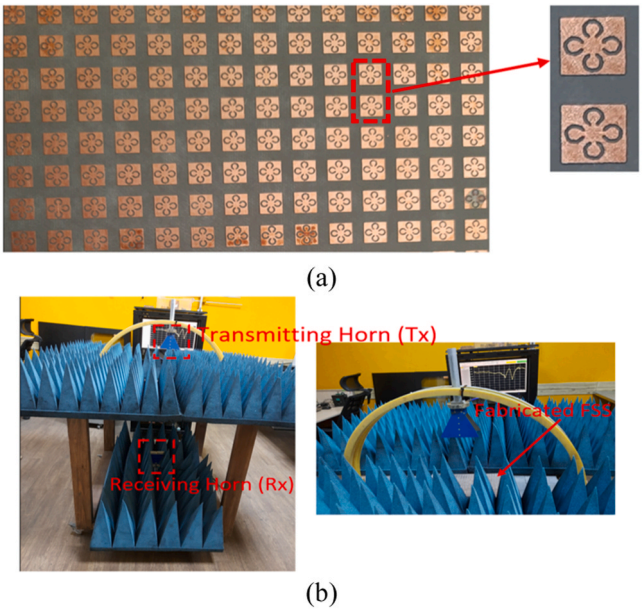

Fig. 8. (a) Fabricated prototype of the presented structure, (b) Measurement set up.

The developments and enhancements in wireless communication systems have rapidly increased the interest in smaller and multifunctional devices. Multi-functionality often brings the need for multi-frequency. Thus, electromagnetic isolation becomes more important. At the point of providing these requirements, closely spaced, dual band, band stop FSSs come into significance. The FSS presented in this study was designed in accordance with these features with dual band-stop response appearing in close locations. In the last few years, the number of studies reporting new FSS designs for 5G mmWave applications have been increased in the literature, but they are either single band or multiband designs with large band ratios [27,28,30]. The rotation symmetrical geometry of the design in [29] demonstrates a single band stop response at 27.84 GHz and leads to reveal identical stopband features for both polarizations. Finally, the outstanding aspects of the presented design will be given in comparison with some previous presented designs having similar features. Table 1 introduces a comparison of the FSS proposed in this study with recently published similar works in the mmWave region. But, only a few closely located dual band FSSs have been reported in 5 G mmWave frequencies. The FSS presented in [28] is designed using two back-to-back resonator layers and provides a band stop response with the band ratio of 1.44. When compared with similar studies, it can be seen that the proposed FSS has other prominent features besides having the smallest band

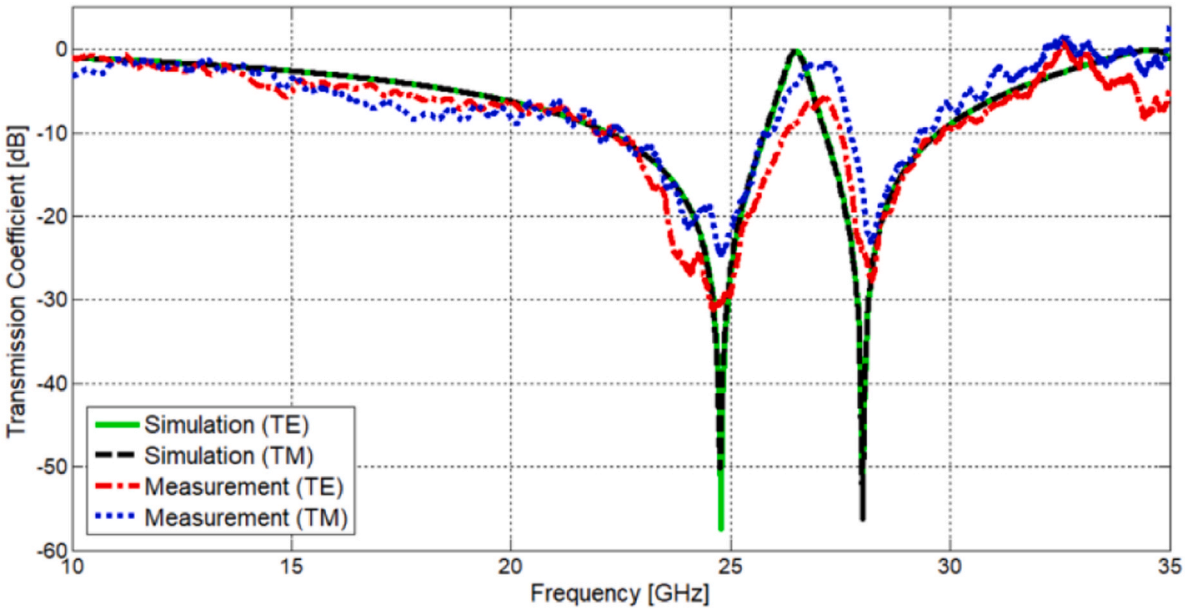

Fig. 9. Simulation and measurement results of the transmission coefficients of the proposed design for both TE and TM polarizations.

Table 1
Comparison of the presented FSS with recent published related FSS designs.

Ref. Year	Resonant frequencies (GHz) & Filter type	Frequency Ratio (f_2/f_1)	Periodicity (λ_l)	Substrate Thickness (λ_l)	BW% (-10 dB)	# of Metal Layer	Resonator Approaches
[23] 2017	28 32.6 Stopband	1.16	0.37	0.077	-	4	Metallic slot layers with four Y-shaped slots in 90° rotation symmetry
[24] 2018	19.52 23.6 31.2 Stopband	1.2 (second/first) 1.36 (third/second)	0.45	0.228	8.8 16.02 6.61	2	Patches with circular loop
[26] 2022	27.2 33.1 Stopband	1.22	0.39	0.092	8.3 13.8	3	Cross loop loaded spiral resonators with wire grid
[27] 2023	24.2 27.7 39.2 Passband	1.14 (second/first) 1.41 (third/second)	0.43	0.040	4.54 5.41 8.93	1	Three slots (circular, octagonal, and sectional square) on a square patch
[28] 2023	27.3 39.2 Stopband	1.44	0.26	0.024	42.8 24.2	2	Back to back resonators
[30] 2023	28 39 Stopband	1.39	0.37	0.070	3.35 2.82	1	Two square rings, with modified T-shaped stubs
This study	24.78 28 Stopband	**1.13**	0.70	0.042	14.48 9.25	1	Four split ring apertures on square patch

where λ_l is the wavelength of the lower operational frequency.

ratio. One of these is the −10 dB stopband fractional BWs with the values of 14.48 % (22.21 GHz-25.80 GHz) and 9.25 % (27.155 GHz-29.746 GHz) and the other is its thin profile. Moreover, having a single layered simple structure is another advantageous feature. It is evident that higher processing technology and manufacturing costs will be required for the fabrication of complex structures. The design in Ref [27] has also a single layer but this FSS provides triple pass bands and has a higher frequency ratio for its transmission blocking bands. The presented FSS owns a simple structure with four split ring apertures loaded square resonator on a single dielectric layer. This makes the designed FSS a viable option for low profile 5G devices.

4. Conclusion

In this study, a novel, single-layer FSS is designed to achieve a closely spaced dual band response for 5G application in the FR2 frequency spectrum. The proposed unit cell is designed with the help of four split ring apertures etched on a square patch, offering stable frequency response in dual polarization due to its rotational symmetry. Under normal incidence, the presented FSS exhibits a dual band, band-stop frequency response at 24.78 GHz and 28 GHz. The resonant frequency ratio of the proposed unit cell is only 1.13. The performance of the fabricated prototype is experimentally validated. Good agreements are obtained between simulated and measured data. Also, the designed structure has the advantages of low cost, simple structure, and ease of fabrication. The proposed design can be applicable in practice such as performance enhancement of antennas, spatial filters, and EMI shielders for the 5G technology.

Declaration of Competing Interest

The authors declare that they have no known competing financial interests or personal relationships that could have appeared to influence the work reported in this paper.

Data availability

No data was used for the research described in the article.

References

[1] M. Xiao, et al., Millimeter wave communications for future mobile networks, IEEE J. Sel. Areas Commun. vol. 35 (9) (2017) 1909–1935.
[2] S. Redana, Ö. Bukaci, 5G PPP Architecture Working Group: View on 5G Architecture, European Commission, ver. 3.0, pp. 1-166, June 2019 [online]. Available: https://5g-ppp.eu/wp-content/uploads/2019.
[3] F.D.L. Coutinho, J.D. Domingues, P.M.C. Marques, S.S. Pereira, H.S. Silva, A.S.R. Oliveira, Towards the flexible and efficient implementation of the 5G-NR RAN physical layer, 2021 IEEE Radio and Wireless Symposium (RWS) (2021) 130–132.
[4] Understanding mmWave for 5G Networks, A 5G Americas white paper, [online]. Available: https://www.5gamericas.org/understanding-millimeter-wave-spectrum-for-5g-networks/, Dec 2020.
[5] ETSI TS 138 101-1 V16.4.0 (2020-07) 5G; NR; User Equipment (UE) radio transmission and reception; Part 1: Range 1 Standalone (3GPP TS 38.101-1 version 16.4.0 Release 16),[online]. Available: http://www.etsi.org/standards-search.
[6] N. Yong, et al., A survey of milimeter wave (mm Wave) communications for 5G: opportunities and challenges, Wirel. Netw. vol. 21 (2015) 2657–2676.
[7] K. Katoch, N. Jaglan, S.D. Gupta, A review on frequency selective surfaces and its applications, 2019 International Conference on Signal Processing and Communication (ICSC) (2019) 75–81, https://doi.org/10.1109/ICSC45622.2019.8938161.
[8] S. Ünaldı, N.B. Tesneli, S. Cimen, A novel miniaturized polarization independent frequency selective surface with uwb response, Radioengineering vol. 27 (4) (2018).
[9] D. Li, T.W. Li, E.P. Li, Y.J. Zhang, A 2.5-D angularly stable frequency selective surface using via based structure for 5G EMI shielding, IEEE Trans. Electromagnetic Compat. vol. 60 (3) (2018).
[10] A. Ghalib, M.U. Khany, M.S. Sharawiz, R. Mittra, A dual-band frequency selective surface for antenna applications in 5G mobile terminals, 2020 IEEE International Symposium on Antennas and Propagation and North American Radio Science Meeting (2020) 765–766.
[11] H. Ullah, F.A. Tahir, M. El-Hadidy, FSS based hexo-fractal dual passband filter for 28 and 38 GHz 5G millimeter-wave communications, 2018 IEEE International Symposium on Antennas and Propagation & USNC/URSI National Radio Science Meeting, Boston, MA, USA (2018) 2365–2366.
[12] Y. Li, P. Ren, Z. Xiang, A dual-passband frequency selective surface for 5G communication, IEEE Antennas and Wireless Propagation Letters vol. 18 (12) (2019) 2597–2601.
[13] B. Decoster, S. Maes, I. Cuiñas, M.G. Sánchez, R. Caldeirinha, J. Verhaevert, Dual-band single-layer fractal frequency selective surface for 5G applications, Electronics vol. 10 (2021) 2880.
[14] S. Ghosh, K.V. Srivastava, An angularly stable dual-band fss with closely spaced resonances using miniaturized unit cell, IEEE Microw. Wirel. Compon. Lett. vol. 27 (3) (2017) 218–220.
[15] N. Wang, T. Du, B. Zhao, A closely located dual-band fss with frequency stability for multi-frequency communication, 2017 International Symposium on Antennas and Propagation (ISAP), Phuket, Thailand (2017).
[16] S. Chen, T. Pan, Y. Lin, Flexible dual-band ultrathin fss with ultra-close band spacing, 2018 International Symposium on Antennas and Propagation (ISAP) (2018).
[17] S. Ünaldı, S. Çimen, G. Cakır, U.E. Ayten, A novel dual-band ultrathin fss with closely settled frequency response, IEEE Antennas Wirel. Propag. Lett. vol. 16 (2017) 1381–1384.
[18] Y. Li, P. Ren, Z. Xiang, B. Xu, R. Chen, Design of dual-stopband fss with tightly spaced frequency response characteristics, IEEE Microw. Wirel. Compon. Lett. vol. 32 (8) (2022) 1011–1014, https://doi.org/10.1109/LMWC.2022.3164070.
[19] B.S. Silva, A.L.P. de Siqueira Campos, M.E.T. Sousa, A.G. Neto, H.D. de Andrade, A tri-band complementary frequency selective surface with very closely spaced resonances, IET Microw. Antennas Propag. vol. 16 (2022) 519–525.
[20] K. Hettak, J. Shaker, Screen-printed dual-band flexible frequency selective surface for 5G applications, 49th European Microwave Conference, Paris, France (1–3) (2019) 519–522.
[21] Z. Zhao, G. Wan, X. Huang, Design of dual-band frequency selective surface with large band ratio for 5G communication, 2020 IEEE 3rd International Conference on Electronics Technology (2020) 756–759.
[22] J. Dong, Y. Ma, Z. Li, J. Mo, A miniaturized quad-stopband frequency selective surface with convoluted and interdigitated stripe based on equivalent circuit model analysis, Micromachines vol.12 (9) (2021) 1027.
[23] Z. Zhao, Y. Yang, H. Huo, J. Li, J. Chen, A. Zhang, A novel dual-band frequency selective surface with close band spacing at Ka-band, 6th Asia-Pacific Conference on Antennas and Propagation (APCAP) (2017).
[24] P. Sharma, et al., Closely spaced tri resonance wide band FSS for S/Ku/Ka band, 2018 IEEE Indian Conference on Antennas and Propogation (InCAP) (2018) 1–5.
[25] B.S. Silva, A.L.P.S. Campos, A. Gomes Neto, Equivalent circuit model for analysis of frequency selective surfaces with ring and double concentric ring apertures, IET Microw. Antennas Propag. vol.7 (14) (2020) 600–607.
[26] S. Dey, S. Dey, S.K. Koul, Second-order, single-band and dual-band bandstop frequency selective surfaces at millimeter wave regime, IEEE Trans. Antennas Propag. vol. 70 (No. 8) (2022) 7282–7287.
[27] S. Gürdal, S. Aksimsek, N.T. Tokan, A triple-band frequency selective surface for 5G millimeter-wave communications, Micro Opt. Technol. Lett. (2023) 1–7.

[28] M.L. Hakim, T. Alam, M.T. Islam, Polarization-insensitive and oblique incident angle stable miniaturized conformal FSS for 28/38 GHz mm-wave band 5G EMI shielding applications, IEEE Antennas Wirel. Propag. Lett. 22 (11) (2023) 2644–2648.
[29] M.L. Hakim, M.T. Islam, T. Alam, Ultra-miniaturized conformal polarization insensitive and incident angle stable FSS for n257 band 5G EMI shielding applications, IEEE Trans. Antennas Propag. (2024) (Early Access).
[30] M. Abdollahvand, E. Martinez-de-Rioja, J.A. Encinar, K. Katoch, Dual-band single-layer frequency selective surface for millimeter-wave 5G applications, 2023 17th European Conference on Antennas and Propagation (EuCAP), Florence, Italy (2023) 1–3, https://doi.org/10.23919/EuCAP57121.2023.10133146.